Original Article

Bulletin of Pure and Applied Sciences.
Vol.37 C (Chemistry), No.1, 2018: P.43-52
Print version ISSN 0970 4620
Online version ISSN 2320 320X
DOI 10.5958/2320-320X.2018.00007.9

Antibacterial studies of polyindole based metal oxide nanocomposites

Dedhila Devadathan[1]*, Baiju V[1], Raveendran R[1]

Author Affiliations
[1]Nanoscience Research Laboratory, Department of Physics, Sree Narayana College, Kollam 691001

Corresponding Author
***Dedhila Devadathan,** Nanoscience Research Laboratory, Department of Physics, Sree Narayana College, Kollam 691001

E-mail: dedhila@yahoo.com

Received on 16th January 2018
Accepted on 28th January 2018

Abstract

In the present work, polyindole based metal oxide nanocomposites were synthesised through chemical oxidation method. For comparative study, the counterparts, polyindole was synthesised through chemical oxidation method and the metal oxides were synthesised through chemical co-precipitation method. Structural studies were done using XRD. Phase purity and crystallinity of these samples were confirmed from XRD. XRD confirmed the formation of nanocomposites. Crystallite sizes were calculated using Scherrer equation for metal oxides. The present study investigates the antimicrobial activity of the synthesized samples as antibacterial agents. The gram positive bacteria: S. epidermidis and C. perfringens, gram negative bacteria: E. coli and V. cholera were the microbes used in the present study. The study confirms that the polyindole based metal oxide nanocomposites samples prepared in the present study showed antibacterial agent activity. The results suggest that proper tuning can make them good antimicrobial agents.

Keywords: Nanoparticles, Antibacterial agents, polyindole,

1. INTRODUCTION

The advances in the field of nanosciences and nanotechnology led to the development of inorganic and organic nanocomposites that are nowadays widely used as antimicrobials. It is a matter of fact that the binding of the particles to the bacteria depends on the surface area available for interaction. Since the reactions takes place at the surface of a chemical or material; the greater the surface for the same volume, the greater will be the reactivity. The smaller size of nanoparticles helps them to easily reach the nuclear content of bacteria which will give more bactericidal effect than the larger particles.

Conducting polymers because of its ability to be doped in reduced or oxidized form (redox properties) has facilitated its usefulness in certain biological applications [1]. Also they can be used in the form of powders, aqueous dispersions and as coatings on variety of substrates. In addition to polymer materials which possess an intrinsic antibacterial activity, these properties can be induced into polymer. This can be achieved through adsorption or coating of an antibacterial agent onto the polymer surface, by direct incorporation of an antibacterial agent into the polymer structure during its synthesis or by immobilization of an antibacterial agent onto the polymer through ionic or covalent bonding [2, 3]. Recent studies indicate that among the polymers inherently showing antibacterial properties includes conducting polymers such as polyaniline. Polyaniline contains quarternary ammonium salts (QAS) and halamines. The antibacterial activity of QAS and halamines are due to the presence of charged nitrogen as well as due to chloride ions. A perfect recipe for making an antibacterial agent is the presence of QAS and halamines [4].

The polymeric matrices are considered as good host materials for metal and metal oxide nanoparticles. They provide additional qualities, such as processability, solubility and thermal stability to the systems formed [5]. Several efforts have been made for fabrication of polymeric material with potential antimicrobial activity [6]. Moreover, the nanocomposites prepared using inorganic metal oxide nanoparticles and organic polymers can find better utilization due to the enhanced antimicrobial activity. All these open the possibility of formulation of a new generation of bactericidal materials. Thus it was thought of interest to study the antimicrobial properties of polyindole having similar structure like PANI and Polypyrrole.

In the present work nickel oxide (NiO), nickel oxide-magnesium oxide (NiO-MgO) and nickel oxide-zinc oxide (NiO-ZnO) was prepared in presence of capping agent, citric acid using co-precipitation method. Polyindole and polyindole based metal oxide nanocomposites were prepared using chemical oxidation method. The aim of the work was to study the variations in the properties of the counterparts when compared to the nanocomposites. The samples synthesizedwas characterized using X-ray Diffraction Spectroscopy (XRD). The present study investigates the antimicrobial activity of the synthesized samples as antibacterial agents. The results of all the samples were also compared.

2. EXPERIMENTAL

AR grade chemicals obtained from Merck were used for the preparation of all the samples. NiO annealed at 500 °C (NF), NiO annealed at 700 °C (NS), NiO–MgO annealed at 500 °C (NMF), NiO–MgO annealed at 700 °C (NMS), NiO–ZnO annealed at 500 °C (NZF) and NiO–ZnO annealed at 700 °C (NZS) were the metal oxide parts prepared in the present study using co-precipitation method. Polyindole (PI) was the conducting polymer selected for the work. Polyindole based NiO (PIN), polyindole based NiO–MgO (PINM) and polyindole based NiO–ZnO (PINZ) were the polyindole based based metal oxides prepared in the present study. PI, PIN, PINM and PINZ were prepared using chemical oxidation method. XRD study was carried out using XPERT–PRO model powder diffractometer (PAN analytical, Netherlands) employing Cu–K_α radiation ($\lambda = 1.54060A^o$) operating at 40kV, 30mA.

3. RESULTS AND DISCUSSIONS

3.1 XRD Analysis

The XRD pattern of PI was found to match well with the XRD patterns in literature [7]. The XRD of polyindole shows the presence of numerous sharp crystalline peaks in the diffraction pattern having 2θ values between 15° and 30°. This can be related to the scattering from bare polymeric chains at the inter-planar spacing. Figure 1 shows the XRD diffraction pattern of PI.

An XRD peak is known to be the measure of crystallinity and the appearance of peaks in the XRD of the polymer confirms the crystalline nature rather than amorphous nature. Higher the degree of regularity in arrangement or ordering of the polymer chain, higher is the crystallinity [8]. The presence of sharp crystalline peaks in the XRD graph indicates good electrostatic (dipole–dipole) interactions among the adjoining molecular chains in the PI matrix and also their highly ordered state [9]. The XRD results justify the PI nanostructures as crystalline in nature.

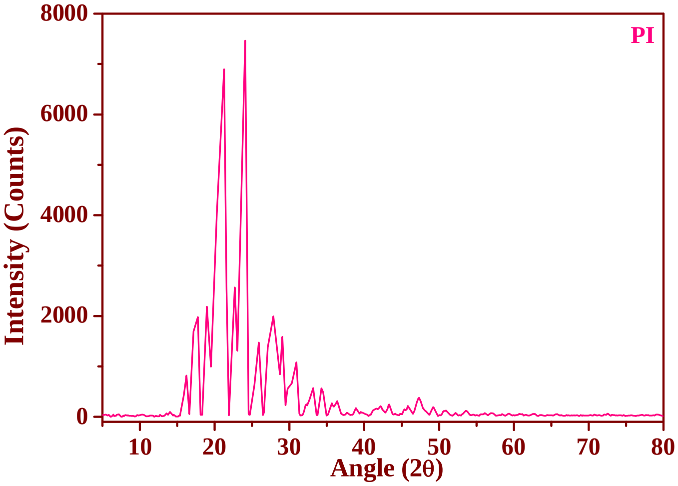

Fig. 1: XRD Spectrum of PI

X-ray diffractograms of NF and NS are shown in Figures 2 and 3 respectively. The well defined X-ray diffraction peaks in the case of NF and NS indicate that NiO formed are crystalline in nature. Also, the diffraction peaks are notably broadened indicating the smaller crystallite size.

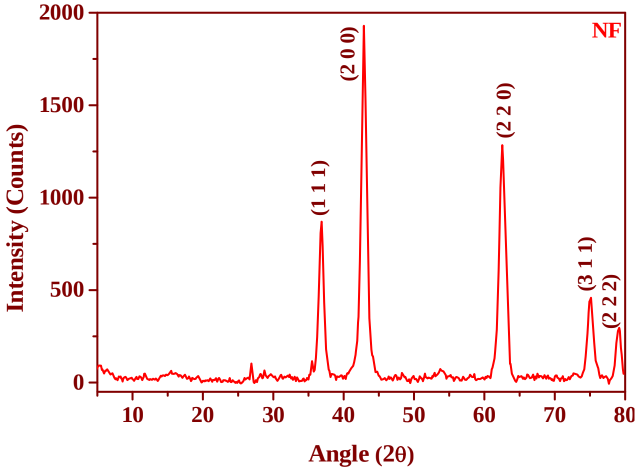

Fig. 2: XRD Spectrum of NF

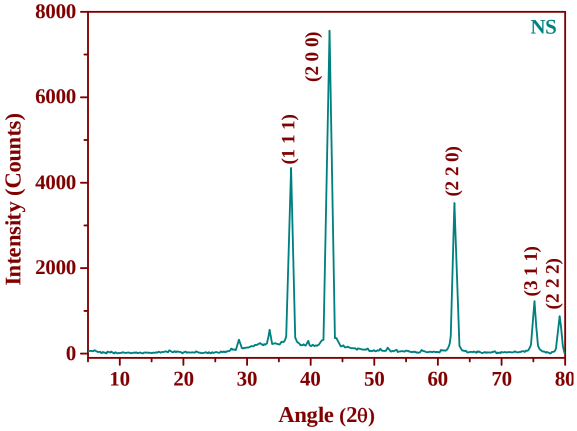

Fig. 3: XRD Spectrum of NS

In order to confirm the phase purity of the samples prepared, the interplanar spacing (d_{hkl} values), 2θ values and relative intensity values corresponding to the observed diffraction peaks were compared with the standard values of NiO reported by JCPDS-International Centre for Diffraction Data. From the comparison of diffraction peaks NF and NS with JCPDS-ICDD pattern number #78-0423 it is clear that NiO formed was a cubic system with FCC lattice.

The average crystallite size were calculated from the line broadening of the XRD pattern, making use of Scherrer formula [10,11] The crystallite size calculated using FWHM (Full width at half maximum) values of five major peaks in the XRD spectrum of NF and NS using Scherrer equation and was found to be 11 nm and 19 nm respectively. It is found that the crystallite size and crystallinity increase with increase in annealing temperature. This is due to agglomeration of particles at higher temperatures.

From the XRD analysis of PIN it is clear that the NiO particles are well distributed in the polymer matrix. The well defined peaks of planes (1 1 1), (2 0 0), (2 2 0) and (3 1 1) and (2 2 2) of NiO were found to be incorporated into the XRD diffraction pattern of polyindole. Also the crystalline peaks in the region between 15° and 30° observed in PIN showed variations when compared to PI which also supports the formation of nanocomposite. Figure 4 shows the XRD pattern of PIN.

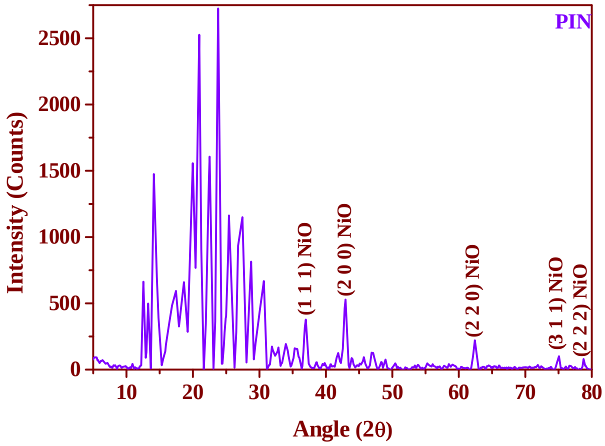

Fig. 4: XRD Spectrum of PIN

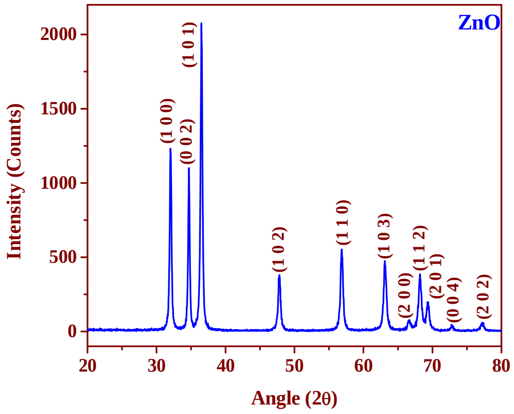

Fig. 5: XRD Spectrum of ZnO

Similar to NF and NS, NZF and NZS also showed well defined X-ray diffraction peaks which indicated that NZF and NZS too had crystalline nature. Again, the broader diffraction peaks indicated the smaller crystallite size. The interplanar spacing (d_{hkl} values), 2θ values and relative intensity values of NZF and NZS corresponding to the observed diffraction peaks were compared with the standard values of NiO and ZnO as reported by JCPDS-International Centre for Diffraction Data. The obtained pattern for ZnO (ZF) was found to match well with JCPDS-ICDD pattern number #79-0205. The data obtained for NiO/ZnO matched with JCPDS-ICDD pattern number #78-0423 of NiO and JCPDS-ICDD pattern number #79-0205 of ZnO separately. From JCPDS, NiO shows cubic system with FCC lattice and ZnO shows hexagonal system with primitive lattice. Figures 6 and 7 show XRD patterns obtained for NZF and NZS respectively.

The variation observed in the d values of the crystal planes in case of NZF and NZS when compared to NiO and ZnO, confirmes the formation of composites. This is also supported by the disappearance of the peak corresponding to (1 0 3) of ZnO in the XRD of the nanocomposite.

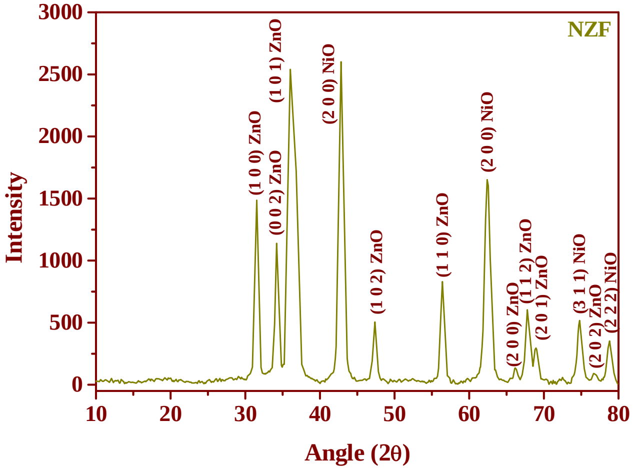

Fig. 6: XRD Spectrum of NZF

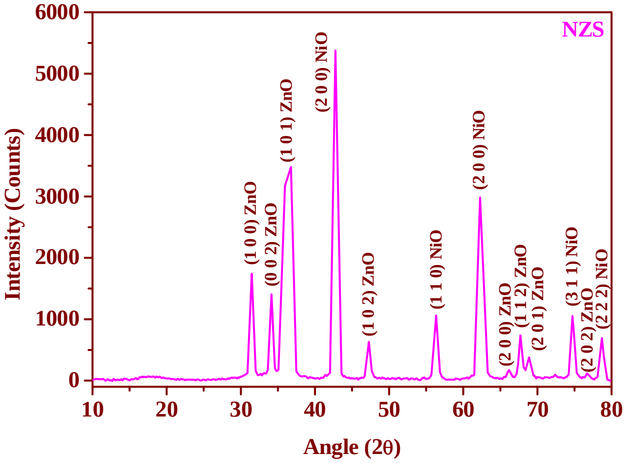

Fig. 7: XRD Spectrum of NZS

The average crystallite size of NZF and NZS calculated from the line broadening of the XRD pattern, using FWHM values of seven major peaks in the XRD spectrum making use of Scherrer formula and was found to be 18 nm and 22 nm respectively. Due to agglomeration of particles at higher temperatures the crystallite size and crystallinity was found to increase with increase in annealing temperature.

XRD of PINZ confirms the formation of nanocomposite. The well defined peaks of planes (1 0 0), (0 0 2) and (1 0 1) of ZnO and (2 0 0), (2 2 0), (3, 1 1) and (2 2 2) of NiO were found to be incorporated into the XRD spectrum of polyindole. It is clear that the metal oxide particles are well distributed in the polymer matrix. Here also the crystalline peaks in the region between 15° and 30° observed in PINZ showed variations when compared to the XRD of PI which also supports the formation of nanocomposite. Figure 8 shows the XRD pattern of PINZ.

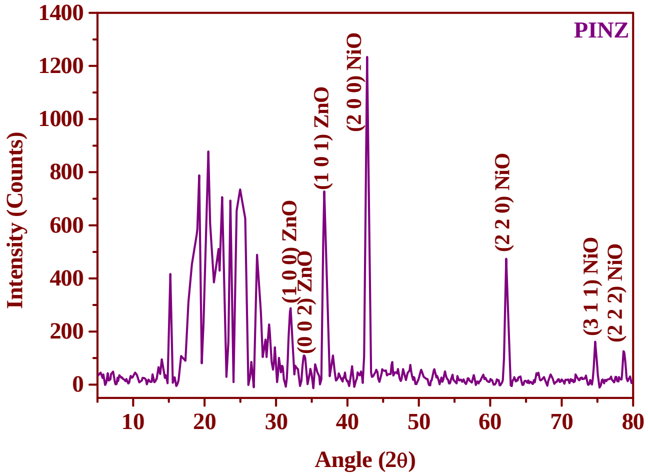

Fig. 8: XRD Spectrum of PINZ

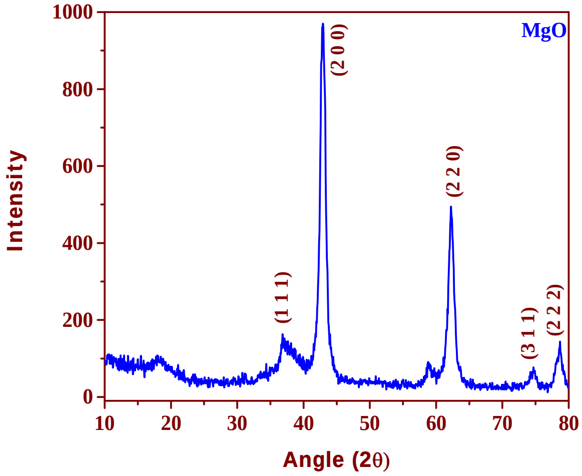

Fig. 9: XRD Spectrum of MgO

NMF and NMS also showed well defined X-ray diffraction peaks which indicated the crystalline nature of NMF and NMS. Here also the broader diffraction peaks obtained indicated the smaller crystallite size. The interplanar spacing (d_{hkl} values), 2θ values and relative intensity values of NMF and NMS corresponding to the observed diffraction peaks were compared with the standard values of NiO and MgO separately. Figure 9 shows XRD diffraction pattern obtained for MgO. The obtained pattern for MgO was found to match well with JCPDS-ICDD pattern number #89-7746. The obtained data for NMF and NMS were matched with JCPDS-ICDD pattern number #78-0423 of NiO and JCPDS-ICDD pattern number #89-7746 of MgO separately. From JCPDS comparison it is clear that MgO like NiO has a cubic system with FCC lattice. Hence it could be concluded that NMF and NMS also formed a cubic system with FCC lattice. Figures 10 and 11 show XRD pattern obtained for NMF and NMS respectively.

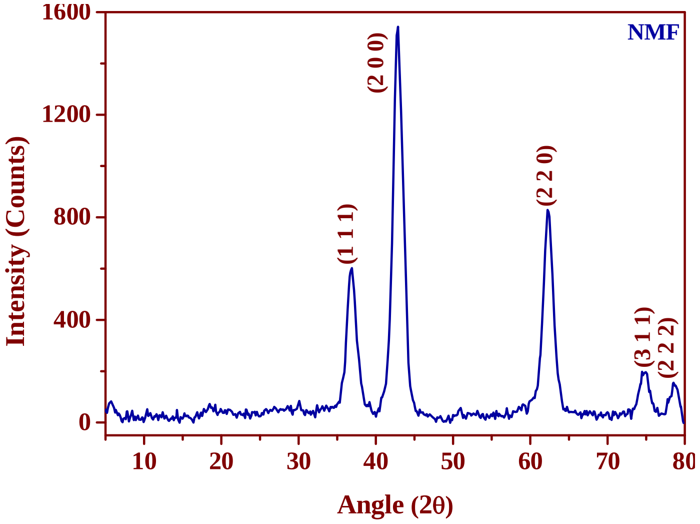

Fig. 10: XRD Spectrum of NMF

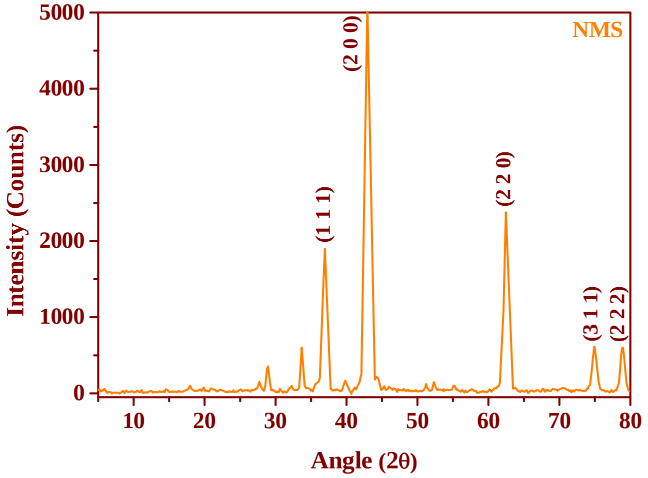

Fig. 11: XRD spectrum of NMS

The average crystallite size of NMF and NMS calculated from the line broadening of the XRD pattern, using FWHM values of three major peaks in the XRD spectrum making use of Scherrer formula and was found to be 6 nm and 16 nm respectively. Due to agglomeration of particles at higher temperatures the crystallite size and crystallinity was found to increase with increase in annealing temperature.

Both NiO and MgO are cubic systems with FCC lattice and the ionic radii of Ni^{2+} and $Mg^{2+}$are also similar. Their lattice parameters are also very close very close. For these reasons, the two oxides can easily form nanocomposite in which the ratio between the components can vary without disturbing the homogeneity. As NMF is formed, the individual XRD peaks of NiO and MgO merges together resulting in the same crystal planes.

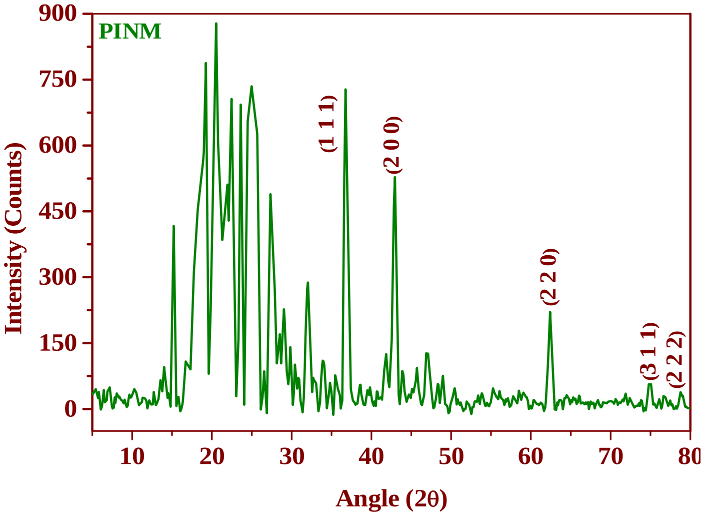

Fig. 12: XRD Spectrum of PINM

XRD of PINM confirms the formation of nanocomposite. The well defined peaks corresponding to the planes (1 1 1), (2 0 0), (2 2 0), (3, 1 1) and (2 2 2) of NiO/MgO were found to be incorporated into the XRD spectrum of polyindole. The variation in the peaks observedin PINM and PI in the region between 15° and 30° supports the formation of nanocomposites. It is clear that the metal oxide particles are well distributed in the polymer matrix. Figure 12 shows the XRD pattern of PINM.

3.2 Antibacterial Studies

The polyindole based metal oxide nanocomposites: PIN, PINZ and PINM showed significant antibacterial effects on the gram positive bacteria: S. epidermidis and C. perfringens, gram negative bacteria: E. coli and V. cholera.

In the case of metal oxides the activity was found to be annealing temperature dependent. The activity of NF was found to higher than NS (Table 1). Similarly the activity of the nanocomposite metal oxides NZF and NMF annealed at 500 °C was found to higher than those of NZS and NMS, the metal oxide nanocomposites annealed at 700 °C (Tables 2 and 3). This decrease in activity of samples annealed at higher temperature can be attributed to decrease in surface to volume ratio due to increase in particle size. The antimicrobial activity of the nanoparticles is generally known to be a function of the surface area which is in contact with the microorganisms. Reactions take place at the surface of a chemical or material. Hence, the smaller size and the higher surface to volume ratio *i.e.*, larger surface area of the NF when compared to NS has enhanced its interaction with the microbes. Table 1 gives the values of zone of inhibition area of NF and NS. Similarly, and NZF and NMF nanocomposites when compared to NZS and NMS have enhanced activity (Table 2 and 3).

Among NF, NZF and NMF the activity was found to be highest for the metal oxide composite, NZF. Here the activity can be attributed to the combined activities of NiO and ZnO. Antimicrobial effects of ZnO nanoparticles can be attributed to several mechanisms:

1. Induction of oxidative stress due to ROS (reactive oxygen species) generation,
2. Membrane disorganization due to accumulation of ZnO nanoparticles in the bacterial membrane and also their cellular internalization,
3. Release of Zn ions that may be responsible for antimicrobial activity by binding to the membrane of microorganisms.

These factors when combined with the activity of Ni^{2+}could have resulted in its higher antimicrobial activity when compared to NF. The zone of inhibition area of NZF is shown in Table 2.

In the case of NMF also the activity was found to be higher than NF. Here the inhibition of microbial growth can be attributed to the combined effect of NiO and MgO. The mechanism of the antibacterial activity of the MgO nanoparticles are mainly attributed to the presence of defects or oxygen vacancies at the surface of the nanoparticles which lead to the lipid peroxidation and reactive oxygen species generation. The activity was higher for NZF. This might be due to the specific activity of NZF to the selected microbes when compared to NMF. Furthermore, other factors such as nanoparticle diffusion rates may also affect bacterial strain differently. The zone of inhibition area of NMF and NMS are given in Table 3.

These materials also being good photocatalysts, their antibacterial mechanism can also be attributed to the destruction of the outer membrane of bacteria by the generated superoxide anion radicals ($\bullet O^{2-}$) as the reactive species. The reactive species such as •OH and $\bullet O^{2-}$ are generated at the catalyst's surface, hence the high surface area is very beneficial for degradation of bacteria. Polyindole prepared in the present study, was found to have significant antimicrobial activity. Like polyailine, polyindole also contains quarternary ammonium salts (QAS) and halamines. Hence the antibacterial activity of PI can be attributed to the activity of QAS and halamines which are present in the polymer chain due to the presence of charged nitrogen as well as due to chloride ions. Nitrogen is present in the PI structure itself and the presence of chloride ions in the polymer chain as dopant. The presence of these two combined with the polycationic nature of polymer and the presence of polyfunctional groups is supposed to be a perfect recipe for making an antibacterial agent.

Table 1: Comparison of Antibacterial and Antifungal activity of NF, NS, PI and PIN

Samples	**E. coli ZOI (mm)**	**C. perfringens ZOI (mm)**	**V. cholerae ZOI (mm)**	**S. epidermidis ZOI (mm)**
NF	10	12	9	13
NS	9	10	7	11
PI	8	9	7	10
PIN	15	18	14	19

Composite of PI with metal oxides; PIN, PINZ and PINM have higher activities when compared to their counter parts. All the factors of PI combined with the activity of metal oxides was found to enhance the activity of the respective nanocomposite. The activity was found to be highest for PINZ than for PINM. Among the polyindole nanocomposites, PIN had lowest activity. The value of zone of inhibition area (ZOI) for PIN is given in Table 1. The corresponding values for PINZ and PINM are given in Table 2 and 3 respectively.

Among the microbes the activity of these samples was highest for S. epidermis and then for C. perfringens. Both these are gram positive bacteria. For all the samples, the activity was highest for gram positive than for gram negative bacteria. Among gram negative bacteria the activity was higher for E. coli than for V. cholerae. The variation in the sensitivity or resistance to both gram positive and gram negative bacteria populations could be due to the differences in the cell structure, physiology, metabolism or degree of contact of organisms with nanoparticles. Gram negative bacteria have a special cell membrane structure which possesses an important ability to resist antimicrobial agents; it has a relatively impermeable lipid based bacterial outer membrane. Greater sensitivity among gram positive bacteria can also be attributed to the greater abundance of amines and carboxyl groups on their cell surface than gram negative bacteria and the greater affinity of the antimicrobials used in the present work towards these groups.

Table 2: Comparison of Antibacterial and Antifungal activity of NZF, NZS, PI and PINZ

Samples	E. coli ZOI (mm)	C. perfringens ZOI (mm)	V. cholerae ZOI (mm)	S. epidermidis ZOI (mm)
NZF	17	19	15	20
NZS	11	13	9	15
PI	8	9	7	10
PINZ	20	23	18	25

Table 3: Comparison of Antibacterial and Antifungal activity of NMF, NMS, PI and PINM

Samples	E. coli ZOI (mm)	C. perfringens ZOI (mm)	V.cholerae ZOI (mm)	S. epidermidis ZOI (mm)
NMF	16	17	13	18
NMS	10	12	8	14
PI	8	9	7	10
PINM	18	20	16	22

4. CONCLUSIONS

The antimicrobial activity of all the synthesized nanocomposites were studied and compared. The results varied considerably. Antimicrobial activity was found to decrease withincrease in particle size in case of metal oxides. The presence quarternary ammonium salts (QAS) and halamines, the polyfunctional group and polycationic nature of polymer chain when combined with the activity of metal oxides enhanced antimicrobial activity of polyindole based metal oxide nanocomposites. The results indicate that both nanometal oxides and nanocomposites are effective against gram positive bacterial strains and gram negative bacterial strains. Activity was found to be highest for gram positive bacteria. Antimicrobial activity was found to be highest for polyindole based NiO/ZnO nanocomposite. Proper tuning of the nanocomposite is expected to improve its antimicrobial activity.

REFERENCES

[1] Peng H, Zhang L, Soeller C and Travas–Sejdic J, Biomaterials, 30, **2009**, 2132–2148.
[2] Bilek F Krizova, T and Lehocky M, Colloids and Surfaces B: Biointerfaces, 88, **2011**, 440–447.
[3] Radheshkumar C and Munstedt H, Mater. Lett., 59, **2005**, 1949–1953.
[4] Seshadri D T and Bhat N V, Indian Journal of Fibre and Textile Research, 30, **2005**, 204–206.
[5] Naka K, Itoh H, Park S and Chujo Y, Poly. Bull., 52, **2004**, 171–176.
[6] Siedenbiedel F and Tiller J C, Polymers, 4, **2012**, 46–71.
[7] Goel S, Advanced Science, Engineering and Medicine, 4, **2012**, 438–441.
[8] Hutten P F V and Hadziioannou G, John Wiley, New York, 3, **1997**, 1–85.
[9] Taylan N B, Sari B and Unal H I, J. Polym. Sci.: Part B: Polym.Phys.,48, **2010**, 1290–1298.
[10] Chen J, Schmidt, Chen J, Wang L, Weidner D J, Zhang J and Wang Y, Journal of Materials Science, 40, **2005**, 5763–5766.
[11] Mattei G, Mazzoldi P, Post M L, Buso D, Guglielmi M and Martucci A, Advanced Materials 19, **2007**, 561–564.